Materials Science Forum Vol. 83-87 (1992) pp. 735-750

DEFECT METASTABILITY IN III-V COMPOUNDS

J. DĄBROWSKI(•) AND M. SCHEFFLER
Fritz-Haber-Institut der Max-Planck-Gesellschaft, Faradayweg 4-6,
D-1000 Berlin 33, Germany

ABSTRACT

Up to very recently the observation of a defect metastability was considered to reflect a rearrangement of a defect *complex*. A substitutional point defect was believed to be structurally stable. In this paper we summarize some recent theoretical studies which show that these assumptions are incorrect, and that point-defect instability is an intrinsic property of *sp*-bonded semiconductors. In particular we summarize the *theoretical indication* that the metastabilities of the famous DX and $EL2$ centers are due to the same basic mechanism, namely the different possibilities of *sp* hybridization. We remind, however, that no *direct* experimental proof of this theoretical prediction exists so far. We also discuss that this type of defect metastability, although a general property of *sp*-bonded systems, may be observable for some centers but not for others.

1. Introduction

Substitutional Ga- or Al-site group-IV impurities in $Al_xGa_{1-x}As$ with $x < 0.22$ are shallow donors, and this also holds for substitutional As-site group-VI impurities. However, in n-type material, and

- when x exceeds 0.22,[1,2]
- or when the sample is put under hydrostatic pressure,[3–6]
- or when the sample is heavily doped,[7,8]

these defects are modified, giving rise to deep centers (with highly localized wave functions), known as DX. The name DX-center was introduced by Lang *et al.*[9,1] in order to suggest that the defect consists of a donor and some additional (unknown) constituent; the DX properties were explained by Lang *et al.*[9,1] in terms of a large lattice relaxation of this complex. In contrast to standard donors, DX centers exhibit a large difference between thermal and optical ionization energies, and, when photoionized at low temperatures, they do not recapture the emitted electrons. The electrons either stay in the conduction band or become metastably trapped in effective-mass states.[10] The first effect is known as persistent photoconductivity and occurs in direct-gap AlGaAs alloys. The second effect is seen in indirect-gap AlGaAs alloys when the lowest conduction-band minimum becomes X.[10]

Another famous defect in GaAs which exhibits a metastability is the $EL2$ center. This is the dominant deep donor in undoped gallium-arsenide crystals grown under As-rich conditions. A most interesting property of $EL2$ is that the transition into the metastable state in which the $EL2$ defect apparently is not observable, can be induced by light ($\hbar\omega \geq 1.18$ eV). The transformation can be redone by heating the sample to $T > 140$ K.[11,12]

At this time there is no general consensus about the microscopic structure of DX and of $EL2$ defects. A unique model, describing the physics of both centers, was developed by Chadi and Chang[13–15] and by us:[12,16–18] Based on parameter-free calculations it was shown that there

is an intrinsic metastability for defects in III-V compounds,[18] which is due to the fact that different defect geometries (the tetrahedral substitutional and a vacancy-interstitial pair) can be stabilized. We should mention that other models for $EL2$ and DX exist as well. The most popular alternatives to the vacancy-interstitial pair model are the following. For $EL2$ some authors emphasize the complex nature of this defect and that the metastability is due to a displacement of an As interstitial.[19–21] For DX some authors argue that the lattice relaxation is in fact small and that the apparent metastability is due to selection rules between different electronic states.[22,23]

A critical test of any of the DX- and $EL2$-center models is the explanation of their metastability. This implies to answer the following questions.

- What is the chemical identity of $EL2$ and of DX?
- What is the basic mechanism of the metastability of $EL2$ and DX centers?
- Under which conditions can one induce the transition to the metastable configuration, and how does the system come back to the ground state?

In this paper we will address these questions by comparing detailed density-functional-theory calculations with available experimental results. In the following Section (Sect. 2) we summarize some aspects of an at-a-first-glance unrelated problem, namely the metastability of graphite $\rightleftharpoons$ diamond carbon. We will argue that the basic mechanism of this metastability, i.e. the nature of sp hybridization, is also responsible for a metastability of sp-bonded defects in III-V compounds. This explanation implies that the basic mechanism of DX and $EL2$ metastabilities is the same, and that this type of defect metastability is a much more general phenomenon than expected so far. In Section 3 we then discuss calculations for the Si donor in GaAs, performed for different hydrostatic pressures. In particular we compare our theoretical results with the most important and most characteristic experimental data of DX. In Section 4 we summarize the theoretical results of the As-antisite in GaAs and its metastability, and Section 5 concludes this paper.

2. The metastability of graphite $\rightleftharpoons$ diamond carbon

The ability of sp-bonded systems to form a variety of different electronic and structural configurations is well known in molecular chemistry as well as for perfect crystals. The most flexible element with this respect is carbon. Its flexibility is particularly pronounced, because the $2p$ valence orbitals – being the first shell of p orbitals – are particularly localized when compared to the valence s orbitals. In view of the purpose of this review an interesting problem is the structure and stability of carbon in the graphite and in the diamond structures. The ground state of crystalline carbon is graphite, but the lifetime of the metastable diamond phase is quite substantial, at least at normal temperatures. To simplify the discussion and to concentrate on the important aspects we show a transition from diamond to the rhombohedral graphite structure. This rhombohedral graphite is not the most common form of graphite, but it is present in normal graphite in concentrations typically between 5 and 15%. Graphite has a planar structure, where different planes are practically uncoupled. Whereas the common form, hexagonal graphite, has a packing as ABAB, rhombohedral graphite has a packing as ABCABC. Different symbols do not imply that the layers are different, but that they are shifted parallel to each other. In Fig. 1 we display the electron density of the diamond structure, and how it changes when it is tranformed to rhombohedral graphite. The total energy per atom is given as well. This theoretical result by Fahy *et al.*[24] shows that for this transition there is a barrier of about 0.3 eV per atom.

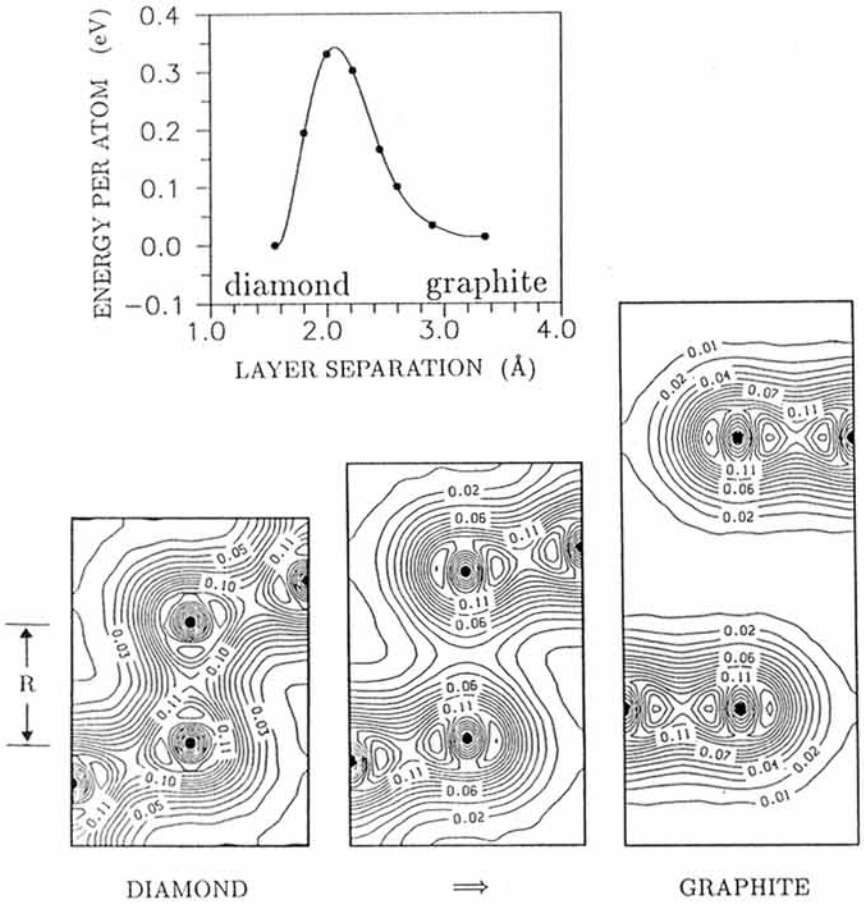

Fig. 1: *Valence-electron density for a calculated phase transition of carbon from diamond (left) to rhombohedral graphite (right). Also shown is the total energy of this transition as a function of the "layer separation" R (after Fahy et al.[24]).*

A further interesting aspect concerns the question what holds the graphite layers so far appart? Srivastava *et al.*[25] recently concluded that this is largely due to the p_z electrons: It was realized that the electronic structure of an isolated graphite layer is quite stiff and each unit cell may be compared to a closed-shell atom. The stiffness of the "closed shell" situation then implies that the main effect of a reduction of the inter-layer distance is the electrostatic repulsion between layers as well as the Pauli repulsion of p_z electrons of different layers. Without the p_z-p_z electron repulsion, the layers would come closer. A strong inter-layer covalent interaction would set in, and a completely different electronic structure would evolve. This is what happens if one calculates boron in the graphite structure, for which the p_z orbitals of an isolated layer are nearly empty.[25]

3. The Si donor in GaAs

We start with a discussion of density-functional theory results of the Si donor in GaAs. Then

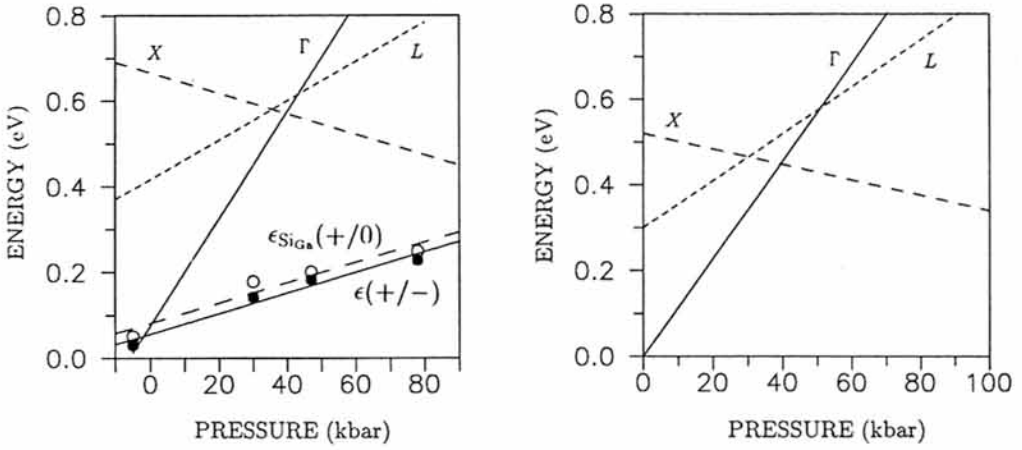

Fig. 2: *Calculated (left) and measured* [1,26] *(right) pressure dependences of the* GaAs *conduction band minima, of the DX level, labeled as* $\epsilon(+/-)$ *[full dots and solid line], and of the deep level of the tetrahedral* Si_{Ga}*, labeled as* $\epsilon_{Si_{Ga}}(+/0)$ *[open dots and dashed line]. The zero of the theoretical pressure scale is adjusted such that the* Γ*-X crossing point is at* 40 *kbar. For the calculated defect levels we neglected lattice relaxation. We also note that the defect levels suffer from the* Γ*-point approximation of the* k *summation. Improving on this we estimate that the* $\epsilon(+/-)$ *line would shift up by about* 0.3 *eV and the* $\epsilon_{Si_{Ga}}(+/0)$ *line would shift up by about* 0.4 *eV.*

we summarize the experimentally known properties of the Si DX center and compare them to the calculations.

3.1 Theoretical results

The density-functional-theory calculations described below were performed for a very accurate basis set ($E^{\rm cut} = 16$ Rydberg), a 54 atom super-cell, and approximating the k-summation by the Γ point. The latter is the main approximation of our studies, which we had to take in most calculations in order to save computer time. Tests for other k-point sets have been performed as well and we will mention these results in the following, whenever they are important. The details of the calculations will be published elsewhere. Because the conduction band, and in particular its changes with pressure or with alloying, play a crucial role for DX properties, we performed calculations at different lattice constants. The calculated equilibrium lattice constant $a_{\rm th} = 5.60$ Å is 1% smaller than the experimental one ($a_{\rm ex} = 5.65$ Å), and the bulk modulus, $B_{\rm th}(a_{\rm th}) = 741$ kbar, is 4% smaller than the experimental one ($B_{\rm ex}(a_{\rm ex}) = 769$ kbar). For the later discussion it is helpful to adjust the zero of the theoretical pressure scale: We will normalize in the following our theoretical pressure scale such that at the conduction band Γ-X crossing point the theoretical pressure agrees with the experimental one (40 kbar). This normalization implies that we add to our *direct* theoretical pressure a value of 31 kbar. In Fig. 2 we compare the experimental and theoretical changes of the conduction band. Note that the theoretical hydrostatic pressure dependences of the conduction band minima are in good agreement with the experimental results. However, as it is well known for converged density-functional-theory calculations, the absolute value of the band gap is too small. Our Γ-point band gap at $p = 0$, using the adjusted pressure scale, is 0.82 eV, whereas the experimental

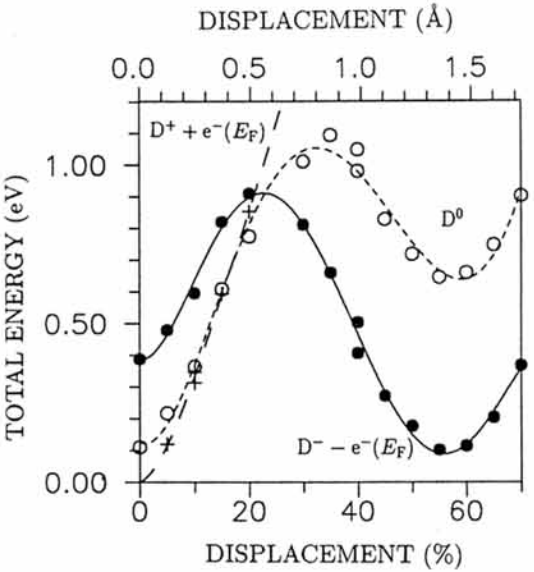

Fig. 3: *Calculated total energy for* GaAs:Si *as a function of the* Si *position. Zero displacement corresponds to the tetrahedral* Si_{Ga} *defect. 100% displacement would correspond to the nearest tetrahedral interstitial position (the corner of the cube shown in Fig.* 4*). Three different charge states are shown. The Fermi level is taken at the minimum of the conduction band, which is at* Γ*. The lattice constant underlying these calculations is* $a = 5.68$ *Å, which corresponds to a pressure of* −5 *kbar (see Fig.* 2 *and text). The main approximations which may affect some quantitative results are the neglect of lattice relaxations and the replacement of the* k *summation by the* Γ*-point.*

optical gap is 1.52 eV.

In Fig. 3 we show the calculated total-energy curves for GaAs:Si, with the Si impurity atom displaced from the tetrahedral substitutional position in the ⟨111⟩ direction. The tetrahedral interstitial position would be at 100% on the scale of Fig. 3, or at the corner of the cube shown in Fig. 4. The results shown in Fig. 3 were obtained with the host atoms frozen at their perfect crystal positions. Lattice relaxations would lower the energies, but we found that the relaxation energy changes only little as a function of the impurity displacement (< 0.2 eV). This would not affect any of our conclusions.

At first we discuss the curve for the negatively charged defect, which is labeled $[D^- - e^-(E_F)]$. We see in Fig. 4 that the minimum of this curve is at a displaced configuration, where the defect symmetry is C_{3v}. Here the defect should be called a vacancy-interstitial (V-I) pair. We emphasize that the Si-interstitial is not at the tetrahedral interstitial site of the lattice but closer to three As atoms. The bonding with these As atoms can be described as largely sp^2 like, and the local geometry resembles that of the graphite structure of carbon (Fig. 1). In fact, the electron densities of the three configurations shown in Fig. 1 and in Fig. 4 look quite similar, although both cases correspond to different systems. Why is the V-I pair stable for $GaAs:Si^-$? Why does the Si not "fall" into the vacancy in order to form a "normal" substitutional defect? We note that only for the negatively charged Si defect the V-I pair geometry has a lower energy than the substitutional, tetrahedral geometry. The mechanism which keeps the impurity at the interstitial side is essentially due to the highest occupied state of the defect. For the V-I

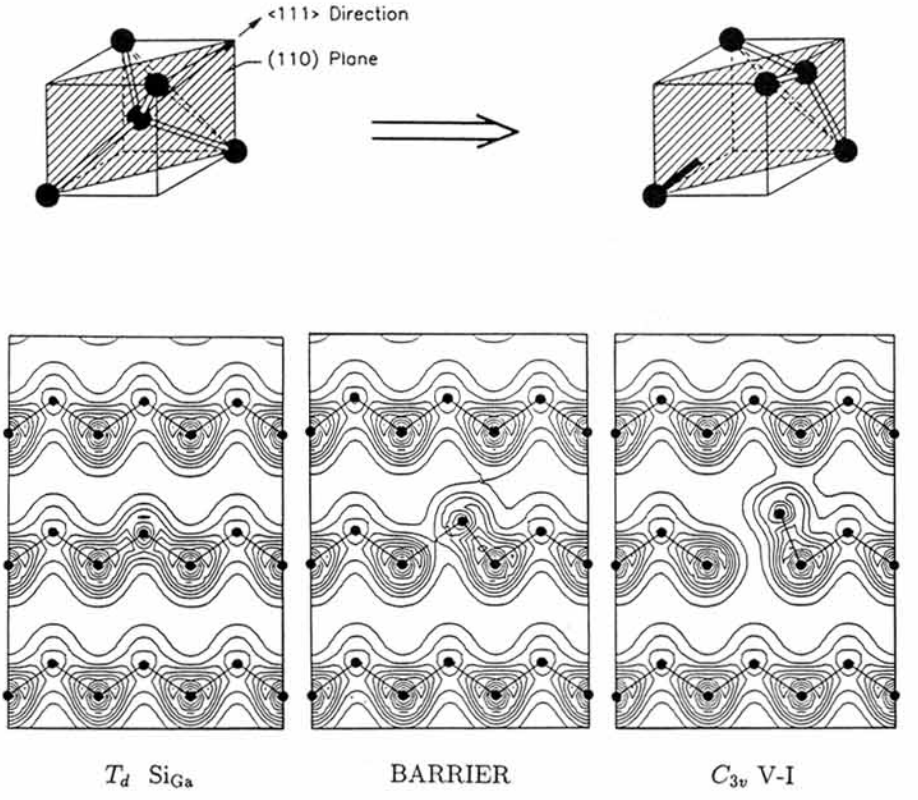

Fig. 4: *The geometry of the tetrahedral* Si_{Ga} *defect (top left) and of the V-I pair (top right), and the valence electron density for* GaAs:Si *at three relevant geometries.*

pair, this state is a single As dangling orbital, indicated in the geometry-plot of Fig. 4 (top right) by the thick black line. It interacts only weakly with the Si interstitial. If the Si atom would be pushed towards the vacant site, this orbital, as well as the Si centered orbitals, will be compressed, which increases the electron kinetic energy. Thus, if these orbitals are filled with electrons, and this is the case for D^-, we get a barrier. The origin of the barrier is thus similar to that of the layer-layer repulsion of graphite (see Section 2). Along the same argument we also understand that if the highest occupied state of D^- would be emptied, as it is the case for the neutral or positively charged defect, the barrier will decrease or vanish.

In Fig. 3 we see indeed that for the neutral system the total-energy curve differs significantly from that of the negatively charged center: For D^0 the stable geometry would be at the tetrahedral position (zero displacement). However, at the V-I pair configuration we can still identify a local minimum. The barrier from this local minimum to the global minimum of D^0 is, however, much smaller than that of the $[D^- - e^-(E_F)]$ curve. We find that the calculated barrier heights depend sensitively on the **k** summation. Improving on the Γ-point approximation we estimate that the theoretical barriers for D^0 and $[D^- - e^-(E_F)]$ for a V-I $\rightarrow$ Si_{Ga} path would be about 0.1 and 0.5 eV, respectively.

If the lattice constant is changed the main effect is a change in the conduction band structure. Assuming that we have n-type conditions, this translates into a change of the Fermi level. As a consequence we obtain a (to first order) rigid shift of the $[D^+ + e^-(E_F)]$ and the $[D^- - e^-(E_F)]$

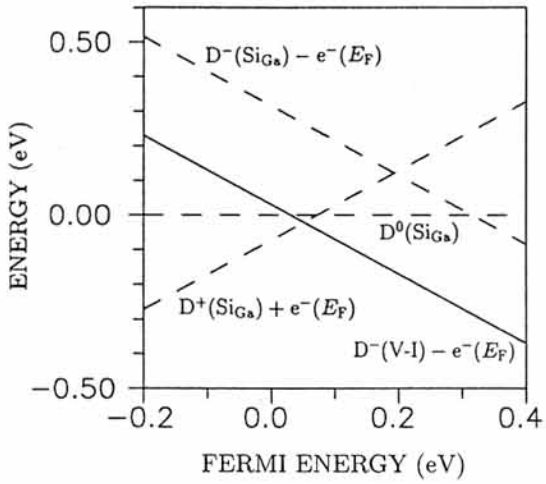

Fig. 5: *Calculated total energies of the single positive, neutral, and single negative charged substitutional* GaAs:Si_{Ga}, *and of the single negative charged V-I pair as a function of the Fermi level.* $E_F = 0$ *is the bottom of the conduction band. The lattice constant underlying these calculations is* $a = 5.68$ *Å, which corresponds to a pressure of* -5 *kbar (see Fig. 2 and text). The main approximations which may affect some quantitative results are the neglect of lattice relaxations and the replacement of the* k *summation by the* Γ*-point.*

curves relatively to the D^0 curve. We find that deformations of the three curves in Fig. 3 with pressure are a second-order effect.

We can induce the metastability also without pressure by changing the Fermi level. If the Fermi level is high, the absolute minimum of the three curves shown in Fig. 3 will be that of the $[D^- - e^-(E_F)]$ curve. Thus, the negatively charged defect with its V-I geometry will be stabilized. If the Fermi level is low, the $[D^+ + e^-(E_F)]$ curve shifts to lower energy and the $[D^- - e^-(E_F)]$ curve shifts to higher energy. Then the minimum of all three possible charge states is that of the positively charged Si substitutional. In Fig. 5 we summarize this discussion in a plot which shows the Fermi-level dependence of the different charge states. This figure also shows the theoretical level positions: The tetrahedral, substitutional Si has transition-state levels $\epsilon_{Si_{Ga}}(+/0) = E_{CB} + 0.1$ eV and $\epsilon_{Si_{Ga}}(0/-) = E_{CB} + 0.3$ eV. Thus, at the lattice constant taken for the calculations in Figs. 3 and 5 both "levels" are resonances in the conduction band. For the V-I pair configuration we obtain $\epsilon_{V\text{-}I}(0/-) = E_{CB} - 0.5$ eV. As we are dealing here with transitions between a mainly valence-band derived state (the highest occupied state of the V-I geometry is essentially a As dangling orbital[12,17]) and the conduction band, these transition-state energies, when compared to experimental ionization energies, may be subject to similar errors as the perfect crystal band gap. Figure 5 shows that the ground state for low Fermi energy is that of $D^+(Si_{Ga})$ and that the ground state for high Fermi energy is that of D^-(V-I). The transition from $D^+(Si_{Ga})$ to D^-(V-I) is direct, i.e. without passing through the neutral configuration. This is what is called a *negative U* behavior: Either there is no electron in the defect induced level, or there are two electrons. The coulombic electron-electron repulsion, which typically implies that energy levels shift to higher energy when the occupation is increased, is more than compensated by the large lattice relaxation, i.e. by the displacement of the Si atom from the substitutional to the V-I pair configuration. The pressure dependence of one half of the energy of the crossing point of the $D^+(Si_{Ga})$ and D^-(V-I) lines of Fig. 5 is

shown in Fig. 2 as the full line, labeled $\epsilon(+/-)$. Figure 2 also shows the pressure dependence of the "normal" Si_{Ga} donor level, $\epsilon_{Si_{Ga}}(+/0)$, as the dashed line.

3.2 Experimental results for the Si *DX* center and comparison with the theoretical results

We now present a list of the experimentally established properties of the Si *DX* center, and we compare these properties to the properties just described in Section 3.1. The experimental results are printed in *italic*, and the properties implied by the theoretical results of Section 3.1 are printed in roman.

1. *The DX center contains only one sort of impurity atom.*[3,4,27–29]
   Obviously, this is in agreement with the theory of Section 3.1, as the only impurity atom is Si.
2. *In GaAs there is only one DX level, while in AlGaAs alloys and in superlattices there are apparently four distinct levels.*[30–35]
   Although in Section 3.1 we were not dealing with an alloy, we can conclude that this experimental result is in agreement with the theoretically predicted geometry of the ⟨111⟩ aligned V-I pair. Morgan[35] had pointed out that alloying changes the second nearest neighbors of the substitutional Si_{Ga}. There are 12 cation atoms in the second shell around a substitutional Si. For each of the four different possibilities of a ⟨111⟩ displaced Si atom there are then four different geometries: There are either 0, 1, 2, or 3 neighbor Ga atoms replaced by Al, and consequently we expect 4 different *DX* levels.
3. *The DX level with respect to the valence-band top, $E_{DX} - E_{VB}$, varies with alloy composition as $(1.78 + 0.57x)$ eV.*[36,33] *For the pressure dependence of $E_{DX} - E_{VB}$ we could not find established data. Results reported by different authors differ quite substantially, ranging from 0 to 10 meV/kbar.*[3–5,27,33,37]
   In Fig. 3 the thermal electron emission is given by a transition from the minimum of the $[D^- - e^-(E_F)]$ to the minimum of the $[D^+ + e^-(E_F)]$ total-energy curve. As this transition corresponds to the emission of two electrons, the thermal binding energy per electron is given by half of this energy difference. This value is shown in Fig. 2 and labeled $\epsilon(+/-)$. The pressure derivative is $d(\epsilon(+/-) - E_{VB})/dp = 2.4$ eV/kbar. Zhang and Chadi[38] obtained 1 meV/kbar. The important point is that the calculated pressure derivative of the $\epsilon(+/-)$ level with respect to the valence-band top is small and very similar to that of the "normal" donor level $\epsilon_{Si_{Ga}}(+/0)$. A comparison of these theoretical pressure derivatives with experiment appears not very meaningful at this time, because of the mentioned scatter of the measured values. Accurate experiments are therefore most important.
4. *The activation energy of electron emission from DX in GaAs varies only very weakly with pressure as $E_e(p) = 300$ meV-1.3meV/kbar $\times p$,*[5] *and it is practically independent of alloy composition.*[36,39,40]
   According to Fig. 3 we expect the following scenario for thermal electron emission. Thermal energy brings the Si atom on the $[D^- - e^-(E_F)]$ total-energy curve from the V-I geometry (55% displacement) to or close to the top of the barrier of this curve. Here the system may emit at first one electron and continue on the D^0 curve, and then emit the second electron. Or it may emit two electrons simultaneously and switch from the $[D^- - e^-(E_F)]$ curve directly to the $[D^+ + e^-(E_F)]$ curve. The activation energy is thus the energy difference between the minimum of the $[D^- - e^-(E_F)]$ curve at 55% displacement and the barrier of this curve. It is difficult to calculate this barrier accurately, because the shape of the total-energy curves in the displacement range from 10 to 40% arises from a crossing (and hybridization) of two different total-energy parabolae (see Ref. 18 and

the discussion of Fig. 6 below). From our calculations we obtain that the main effect of pressure is that it changes the conduction band structure and (in n-type material) the Fermi level. Thus the two curves for the positive and for the negative charge state in Fig. 3 are shifted, but the shape of each curve is only slightly modified. This implies that the activation energy is not much affected by pressure. We estimate that it should change as -4 meV/kbar, but we emphasize that this is not a very accurate estimate.

5. *The optical ionization energy, $E_o = 1.4$ eV, is much larger than the thermal ionization energy,*[41] *and it is practically independent of the alloy composition.*[41]
For the optical excitation from the deep level of the negatively charged V-I pair the calculations give 0.6 eV (see Fig. 3), and this value increases with pressure as 11.5 meV/kbar $\times p$. Thus the calculated optical ionization energy is much larger than the thermal ionization energy. We like to remind that the optical excitation energy from a deep level, which has mainly As dangling-orbital character, to the conduction band may be subject to similar errors as the calculated band gap. This concerns mainly the absolute value of the optical ionization energy. The pressure dependence should be less affected by this band-gap problem. Unfortunately, the experimental uncertainty is too large to compare a measured pressure dependence of E_o with the calculated 11.5 meV/kbar.
Recently a two-step photo ionization of DX(Te) was reported by Dobaszewski and Kaczor.[42]
These results are qualitatively in accord with our total-energy curves of Si shown in Fig. 3.

6. *The electron-capture cross section is small and thermally activated.*[9]
The theoretical results of Fig. 3 strongly suggest that the scenario of capture is as follows. If the defect is in the positively charged state and in the tetrahedral configuration, the transformation to the V-I configuration requires the capture of two electrons. A simultaneous capture of two electrons in a conduction-band resonance is unlikely, and still some thermal energy would be needed to overcome the barrier of the $[D^- + e^-(E_F)]$ curve. Instead, we expect that the system will at first capture only one electron. This brings us on the D^0 curve. Thermal vibrations then displace the Si atom. If this displacement is larger than about 25%, the system will capture the second electron. The concerted nature of this $Si_{Ga}^+ \rightarrow$ V-I^- structural transition strongly suggests that electron capture at low temperature has low probability.
Additional experiments show that in indirect-band-gap AlGaAs the photoexcited electrons can be trapped in non-DX states.[43,10]
In these experimental papers it was argued that this trapping occurs in the X-minimum effective-mass state. According to our calculations, this is certainly possible. However, the calculations also indicate a second possibility. In GaAs under high pressure, also the "normal" deep level of Si_{Ga} becomes a bound state[17] (see Fig. 2), and this will also happen in indirect-gap AlGaAs. We suggest that this "normal" Si_{Ga} state can be responsible for the observed trapping in some pressure range.

7. *The capture rate depends exponentially on the quasi Fermi level, which was interpreted that electron capture goes via an intermediate state.*[44,45]
This interpretation is fully supported by the calculations (see Fig. 3) and the scenario suggested by them (see the discussion under No. 6).

8. *The electron-capture barrier exhibits a pronounced minimum with alloy composition at $x = 0.37$.*[7,36,46]
In the theoretical model (see No. 6 above) the electron-capture is determined by the $\epsilon_{Si_{Ga}}(+/0)$ level of Fig. 2. As noted, this level is involved in the first step of the capture process. Therefore, the barrier depends on the position of this level with respect to the Fermi level (or, precisely, the quasi-Fermi level for electrons), which in n-type material follows the conduction band edge. The difference $\epsilon_{Si_{Ga}}(+/0) - E_F$ has practically the same shape as the measured electron-capture barrier of DX centers.

9. *Studies of hot-electron capture by DX centers in GaAs/AlGaAs heterojunctions show that the capture process goes via an intermediate state. This intermediate state, which is possibly an excited state of Si^0_{Ga}, is separated from the ground state of DX by a barrier E_b, where E_b is nearly independent of alloy composition.*[47]
The results of Fig. 3 suggest that electrons may be captured at the tetrahedral Si_{Ga} center: $[D^+(Si_{Ga}) + e^-_{hot}] \rightarrow D^0(Si_{Ga})$. This process will become efficient for voltages higher than a threshold voltage V^0 i.e. for voltages high enough to provide hot electrons with energy above the $\epsilon_{Si_{Ga}}(+/0)$ level. The threshold voltage V^0 should depend on pressure, on alloy composition, and on the position of the $\epsilon_{Si_{Ga}}(+/0)$ level. When measured at V^0, the barrier between $D^0(Si_{Ga})$ and the $[D^-(V\text{-}I) - e^-_{hot}]$ is an intrinsic property of the defect and should only weakly depend on pressure or alloy composition.
10. *At low temperature, the cross section for hole capture by DX is several orders of magnitude larger than the cross section for thermal electron capture.*[48,49]
The details of how a hole is captured by the negatively charged V-I pair depend on the relative positions of the total-energy curves of $[D^- + h^+_{VB}]$ and of D^0. In particular, a dependence on the band gap (i.e. on pressure or alloy composition) is expected. Hole capture is a direct process and not a concerted process as electron capture (see the discussion at No. 6 above). Therefore, the hole capture process should have a much larger cross-section. Moreover, we would like to mention that while at higher temperatures the neutral center automatically emits its electron to the conduction band, our results suggest that at low temperatures the neutral V-I configuration becomes stabilized (Fig. 3). It means that another hole has to be captured in order to transform the defect to the tetrahedral configuration. Thus, at low temperatures we would expect two different cross sections for hole capture: For the $[D^-(V\text{-}I) + h^+_{VB}] \rightarrow D^0(V\text{-}I)$ process and for the $[D^0(V\text{-}I) + h^+_{VB}] \rightarrow D^+(Si_{Ga})$ process.

In summary we find that many *DX* properties can be explained by the V-I model of Section 3.1. The change in nature of the defect GaAs:Si from a shallow to deep center is essentially due to a change of the Si position which is induced by a change of the (quasi) Fermi level. Several experimental results are directly explained by the calculations. However, some questions remain which call for more accurate experiments as well as for more accurate calculations. These are in particular related to the above items No. 3, 4 and 5. In addition we note that susceptibility measurements seem to indicate that *DX* centers are paramagnetic.[50] This is not confirmed by EPR and in fact it has been questioned by other studies.[51] Paramagnetism *of the ground state* of *DX* centers would be in conflict with the V-I model. A more detailed experimental and theoretical study of these points should help to finally confirm, to reject, to refine the model of Section 3.1.

4. Anion antisite defects in GaAs

In this Section we summarize some aspects of our earlier work[12,16,18] on anion antisite and antisite-like defects in III-V compounds. An anion antisite defect in GaAs is created when a group-V atom substitutes a Ga atom. In difference to the single donor Si_{Ga}, which we discussed in Section 3, these defects are double donors. Nevertheless, we find some very similar properties. There is, however, one additional and very interesting aspect predicted by the calculations for some anion antisites, namely the possibility to transform the defect from the stable to the metastable geometry by an optical excitation, without changing the defect charge state.

From a simple tight-binding model (where atomic orbitals of the substitutional atom hybridize with the dangling orbitals of the cation vacancy[53,54]) we expect the electronic structure of the tetrahedral anion antisite to have a deep bound state of a_1 symmetry, and above it a state of t_2

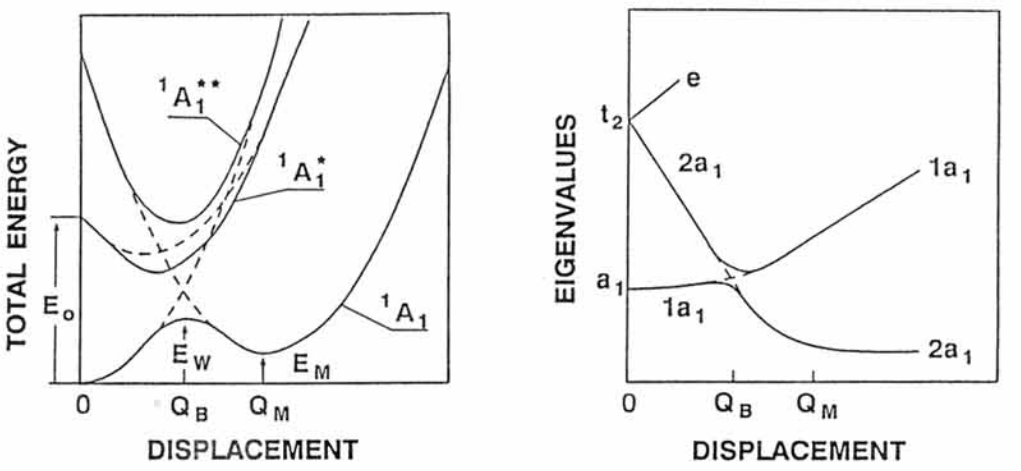

Fig. 6: *Schematic figure of total energies for the ground and excited electronic configurations (left) and single-particle energies (right) as function of the displacement of the defect atom along the* ⟨111⟩ *axis. Typical values of the* a_1-t_2 *splitting at zero displacement and of* E_o *are of the order of* 1 *eV.*

symmetry. For the As_{Ga} antisite the a_1 eigenvalue is at mid gap, and the donor level involves a population change of this a_1 state. The t_2 state is found in the conduction band, giving rise to a rather sharp resonance below the L minimum. The sharpness of this resonance is due to the fact that the electron density in GaAs (at zero pressure) between the Γ and L conduction-band minima is rather low.

Figure 6 gives a schematic summary of the total energy as well as of the relevant eigenvalues of anion antisite and antisite-like defects in III-V compounds.[18] As in Fig. 3 (Section 3.1), zero displacement refers to the tetrahedral, substitutional defect. The just mentioned a_1 and t_2 single-particle eigenvalues can be identified on the right part of Fig. 6 at zero displacement. The displacement of the defect atom along the ⟨111⟩ direction towards the interstitial site lowers the local symmetry to C_{3v}, and the t_2 state splits: $t_2 \rightarrow a_1 + e$. The T_d symmetry a_1 state is now labeled $1a_1$, and the a_1 component of the T_d symmetry t_2 state is labeled $2a_1$. The three lowest-energy mean-field configurations of the A_1 representation are then $(1a_1{}^2 2a_1{}^0)$, $(1a_1{}^1 2a_1{}^1)$ and $(1a_1{}^0 2a_1{}^2)$. For small displacements Q the energy of the ground state exhibits a parabolic behavior around the minimum at the $Q = 0$ geometry, and is dominated by the configuration $(1a_1{}^2 2a_1{}^0)$. With larger displacement, the eigenvalue difference $\epsilon(2a_1) - \epsilon(1a_1)$ decreases and the interaction between the three configurations increases until we reach an anticrossing point which results in the local maximum of the ground-state energy. In this process the occupied a_1 state localizes and evolves into a cation vacancy like dangling-bond state. Further displacements bring all antisite defects to a metastable configuration, at a displacement of $1.2 - 1.4$ Å from the substitutional site.

The resulting total-energy surface for the neutral center (see the $^1A_1$ curve in the Fig. 6) resembles closely the D^- curve of Fig. 3. In fact, a neutral anion antisite should be compared to a negatively charged Si donor, because the energy barrier between the metastable and stable geometries arises from the double occupancy of the $2a_1$ state (see the discussion in Section 3.1). The main difference of neutral anion antisites when compared to Si is that the global minimum of GaAs:As (and of other group V defects) is at the tetrahedral substitutional configuration

($Q = 0$), i.e., the V-I pair configuration (at Q_M) is metastable. The physics behind this total-energy curve, i.e. its qualitative shape with two minima, can be understood along the same arguments which were given in Section 3.1. Removing one or two electrons from the neutral anion antisite would make the V-I geometry energetically more unfavorable and would reduce or eliminate the barrier between the V-I and the normal substitutional geometries.

As Fig. 6 shows, there is an interesting excited many-electron state (electronic configuration $1a_1^1 2a_1^1$) which is labeled $^1A_1^*$. This state can be reached from the ground state (electronic configuration $1a_1^2 2a_1^0$) by optical excitation. At the terahedral geometry ($Q = 0$) this configuration is unstable with respect to a Jahn-Teller distortion. As a consequence, this excited $^1A_1^*$ state may provide a channel for an optically inducible structural transition.[55] Figure 6 (left side) indicates that the system may displace sufficiently far on this $^1A_1^*$ total-energy curve so that the defect atom, when it deexcites, "falls" to the other side of the barrier, thus ending in the V-I configuration. At low temperatures this geometry will be frozen in. For a reasonable probability of this optically inducible transition it is necessary that the energy of the excited state $^1A_1^*(Q = 0)$ is *above* the local maximum of $^1A_1(Q = Q_B)$. In GaAs, Caldas *et al.*[18] found this condition fulfilled for the As and P antisites, but not for the Sb antisite.

The similarities and differences of the metastable properties of the silicon donor and the cation-site double donors can be summarized as follows.

1. When the deep a_1 state is occupied with two electrons, the substitutional and the V-I atomic configurations are close in energy and separated by an energy barrier.
2. When the deep a_1 state is empty or occupied by only one electron, this barrier vanishes or is significantly reduced.
3. The highest occupied state of the V-I configuration is very localized. It resembles an arsenic dangling orbital.
4. It depends on the defect, which of the two total-energy minima in the two-electron state (the substitutional or the V-I geometry) is the lowest one.
5. Donor levels of the V-I configuration are considerably closer to the valence band than donor levels of the tetrahedral substitutional configuration.
6. The substitutional $\rightleftharpoons$ V-I metastability will be inducible by light for some centers, but not for others.

A detailled comparison between the calculated properties of anion antisite defects in III-V crystals is possible for GaAs:As_{Ga}. This center has attracted special attention in recent years because of its role in the $EL2$ defect. We believe that the electronic and structural properties of the As_{Ga} and the corresponding V-I pair explain the properties of $EL2$. A detailled comparison with the experimental properties of $EL2$ had been given elsewhere[12,52] and will not be repeated here. We like to address, however, some open questions which remain. For the *paramagnetic* antisite for which the highest occupied level is occupied with only one electron it was reported[19,20] that the As_{Ga} is paired with an As interstitial. This has been already briefly discussed in Ref. 12. It is not clear if in thermal equilibrium this interstitial is present also close to the neutral As_{Ga} and if it plays a significant role in the structural transition. For the *paramagnetic* anion antisite the calculations reported above require that the transition into the metastable geometry is a two step process: 1) capture of one electron ($As_{Ga}^+ \rightarrow As_{Ga}^0$) and then the optical excitation of the neutral antisite. If the interstitial is more relevant in the first or in the second step or of it effects the lifetime of the neutral charge state is not clear at this time. More experiments are needed to answer these questions. A further aspect which we feel is not fully understood concerns the optical absorption of $EL2$ (which we identify with the neutral As_{Ga}^0 center) and of the paramagnetic As_{Ga}^+ antisite. The internal absorption of the two centers

(which we identify with the $a_1^2 t_2^0 \rightarrow a_1^1 t_2^1$ and the $a_1^1 t_2^0 \rightarrow a_1^0 t_2^1$ excitations, respectively) appears to be significantly more pronounced for $EL2$ than for the paramagnetic antisite. It would be interesting to understand the reason for this difference.

5. Summary

Above we described results of elaborate electronic structure, total energies and forces calculations for cation-site single and double donors in III-V crystals. The calculations predict a new type of defect metastability which in many ways resembles that of the diamond $\rightleftharpoons$ graphite metastability of carbon. Thus, the basic mechanism is the ability of sp bonded systems to bind in different mixtures of the s and p valence orbitals (e.g. sp^3 and sp^2). Different forms of sp hybridizations stabilize different local geometries (sp^3: fourfold coordinated/T_d, sp^2: threefold coordinated/C_{3v}). Therefore, it can be possible to induce a structural transition from the tetrahedral (sp^3 bonding) to the trigonal (largely sp^2 bonding) geometry by an electronic excitation. We cannot predict, however, without a full calculation, for which defects this metastability will be relevant and if or how the transition from the stable to the metastable geometry can be induced by electronic excitations with significant probability: The lifetime of the excited state, the height of the barrier and the energy difference between the stable and the metastable geometries will be different for different defect atoms and for different host crystals.

Although the detailled calculations reported in this paper were concerned with cation-site donors, where the metastability is due to a displacement of the defect atom, we note that the same type of process can also occur for anion-site donors[14,15]. Here, however, the nearest neighbor cation moves.

The theoretical results for the electronic structures and the total-energy curves for all relevant charge states and the physical consequences implied by these results are compared with a variety of experimental investigations of $EL2$ and DX centers. In all cases where the experimental results are well established, agreement with the theoretical prediction is found. As this comparison implies a variety of different properties, such as optical, thermal, and magnetic properties, it strongly suggests that the basic mechanism described by the theory is in fact the relevant one. Although this comparison between theoretical predictions and experimental properties is highly suggestive it should not yet be judged as a *final scientific proof* of the chemical identity and the atomic structure of $EL2$ and DX, and of the operative mechanism of their metastability. Instead we hope that our contribution stimulates more experimental investigations which finally will confirm, reject, or refine the V-I model. Some experiments which we feel would be important are mentioned in the above discussion in Sections 3.2 and 4. We also noted the main approximations of the calculations. This mainly concerns the DX study. The main approximations beeing the neglect of lattice relaxations of the host crystal and the Γ point approximation of the $\mathbf{k}$ summation. The influence of these approximations has been studied for some geometries so that an estimate could be given of how they affect the theoretical results.

Acknowledgement

We acknowledge a pleasant collaboration with M.J. Caldas, A. Fazzio, R. Strehlow, G.P. Srivastava, and R. Stumpf on some aspects discussed in this paper. We thank T.N. Morgan and J. Schneider for several stimulating discussions which significantly helped us to develop our current understanding of point-defect metastability. Part of this work was supported by the Volkswagenstiftung.

References

(*) Permanent address: Instytut Fizyki PAN, Al. Lotników 32, 02-668 Warszawa, Poland

1. D.V. Lang, R.A. Logan, and M. Jaros, Phys. Rev. B **19**, 1015 (1979).
2. P.M. Mooney, Semiconductors Science and Technology, to be published.
3. M. Mizuta, M. Tachikawa, H. Kukimoto, and S. Minomura, Jpn. J. Appl. Phys. **24**, L143 (1985).
4. M. Tachikawa, T. Fujisawa, H. Kukimoto, A. Shibata, K. Oomi, and S. Minomura, Jpn. J. Appl. Phys. **24**, L893 (1985).
5. M.F. Li, P.Y. Yu, E.R. Weber, and W. Hansen, Appl. Phys. Lett. **51**, 349 (1987).
6. M.F. Li, P.Y. Yu, E.R. Weber, and W. Hansen, Phys. Rev. B **36**, 4531 (1987).
7. E. Calleja, A. Gomez, and E. Munoz, Appl. Phys. Lett. **52**, 383 (1988).
8. T. Fujisawa, J. Yoshino, and H. Kukimoto, Jpn. J. Appl. Phys. **29**, L388 (1990).
9. D.V. Lang and R.A. Logan, Phys. Rev. Lett. **39**, 635 (1977).
10. J.E. Dmochowski, L. Dobaczewski, J.M. Langer, and W. Jantsch, Phys. Rev. B **40**, 9671 (1989).
11. G.M. Martin, and S. Makram-Ebeid, in *Deep Centers in Semiconductors*, edited by S.T. Pantelides (Gordon and Breach, New York, 1986), p. 231.
12. J. Dąbrowski and M. Scheffler, Phys. Rev. Lett. **60**, 2183 (1988); Phys. Rev. B **40**, 10391 (1989).
13. D.J. Chadi and K.J. Chang, Phys. Rev. Lett. **60**, 2187 (1988).
14. D.J. Chadi and K.J. Chang, Phys. Rev. Lett. **61**, 873 (1988).
15. D.J. Chadi and K.J. Chang, Phys. Rev. B **39**, 10063 (1989).
16. M. Scheffler, in *Festkörperprobleme XXIX (Advances in Solid State Physics)*, edited by U. Rössler (Vieweg, Braunschweig, 1989), p. 231.
17. J. Dąbrowski, M. Scheffler, and R. Strehlow, in *Proceedings of ICPS-20*, edited by E.M. Anastassakis and J.D. Joannopoulos (World Scientific, Singapore, 1990), p. 489.
18. M.J. Caldas, J. Dąbrowski, A. Fazzio, and M. Scheffler, Phys. Rev. Lett. **65**, 2046 (1990); and in *Proceedings of ICPS-20*, edited by E.M. Anastassakis and J.D. Joannopoulos (World Scientific, Singapore, 1990), p. 469.
19. H.J. von Bardeleben, D. Stievenard, D. Deresmes, A. Huber, and J.C. Bourgoin, Phys. Rev. B **34**, 7192 (1986).
20. B.K. Meyer, D.M. Hofmann, J.R. Niklas, and J.-M. Spaeth, Phys. Rev. B **36**, 1332 (1987).
21. C. Delerue, M. Lannoo, D. Stievenard, H.J. von Bardeleben, and J.C. Bourgoin, Phys. Rev. Lett. **59**, 2875 (1987).
22. H.P. Hjalmarson and T.J. Drummond, Appl. Phys. Lett. **48**, 656 (1986).
23. J.C. Bourgoin and A. Mauger, Appl. Phys. Lett. **53**, 749 (1989).
24. S. Fahy, S.G. Louie, and M. Cohen, Phys. Rev. B **34**, 1191 (1986).
25. G.P. Srivastava, R. Stumpf, and M. Scheffler, unpublished (1991).
26. Landoldt-Börnstein: Numerical Data and Functional Relationships in Science and Technology, New Series Group III (Springer, New York 1982), Vol. 17a and 22a, and references therein.

27. D.K. Maude, J.C. Portal, L. Dmowski, T.J. Foster, E. Eaves, M. Nathan, M. Heiblum, J.J. Harris, and R.B. Beall, Phys. Rev. Lett. **59**, 815 (1987).

28. L. Eaves, T.J. Foster, D.K. Maude, J.C. Portal, R. Murray, R.C. Newman, L. Dmowski, R.B. Beall, J.J. Harris, M.I. Nathan, and M. Heiblum, Inst. Phys. Conf. Ser. **95**, 315 (1989).

29. P.M. Mooney, Appl. Phys. Reviews, J. Appl. Phys. **67**, R1 (1990).

30. P.M. Mooney, T.N. Theis, and S.L. Wright, Appl. Phys. Lett. **53**, 2546 (1988).

31. R.L. Piotrzkowski, T. Suski, P. Wiśniewski, K. Ploog, and L. Knecht, J. Appl. Phys. **68** 3377 (1990).

32. T. Baba, M. Mizuta, and T. Fujisawa, J. Yoshino, and H. Kukimoto, Jpn. J. Appl. Phys. **28**, L891 (1989).

33. Z. Wilamowski, J. Kossut, W. Jantsch, and G. Ostermayer, Semiconductors Science and Technology, to be published.

34. P.M. Mooney, T.N. Theis, and E. Calleja, Journal of Electronic Materials **20**, 23 (1991).

35. T.N. Morgan, Journal of Electronic Materials **20**, 63 (1991).

36. P.M. Mooney, N.S. Caswell, and S.L. Wright, J. Appl. Phys. **62**, 4786 (1987).

37. J.E Dmochowski, P.D. Wang, and R.A. Stadling, in *Proceedings of ICPS-20*, edited by E.M. Anastassakis and J.D. Joannopoulos (World Scientific, Singapore, 1990), p. 658.

38. S.B. Zhang and D.J. Chadi, Phys. Rev. B **42**, 7174 (1990).

39. E. Calleja, F. Garcia, A. Gomez, E. Munoz, P.M. Mooney, T.N. Morgan, and S.L. Wright, Appl. Phys. Lett. **56**, 934 (1990).

40. T.N. Theis and P.M. Mooney, Mater. Res. Soc. Symp. Proc. **163**, 729 (1990).

41. P.M. Mooney, G.A. Northrop, T.N. Morgan, and H.G. Grimmeiss, Phys. Rev. B **37**, 8298 (1988).

42. L. Dobaczewski and P. Kaczor, Phys. Rev. Lett. **66**, 68 (1991).

43. J.E. Dmochowski, J.M. Langer, J. Raczyńska, and W. Jantsch, Phys. Rev. B **38**, 3276 (1988).

44. T.N. Theis, T.N. Morgan, B.D. Parker, and S.L. Wright, Materials Science Forum **38-41**, (Trans Tech Publications, Switzerland, 1989) p. 1073.

45. W. Jantsch, Z. Wilamowski, and G. Ostermayer, Semiconductors Science and Technology, to be published.

46. P.M. Mooney, H. Calleja, S.L. Wright, and M. Heiblum, in *Defects in Semiconductors*, edited by H.J. von Bardeleben (Trans Tech Publications, Switzerland, 1986) p. 417.

47. T.N. Theis, B.D Parker, P.M. Solomon, and S.L. Wright, Appl. Phys. Lett. **49**, 1542 (1986); T.N. Theis and B.D Parker, Appl. Surf. Science **30**, 52 (1987).

48. M.O. Watanabe, Y. Ahizawa, N. Sugiyama, and T. Nakanisi, Inst. Phys. Conf. Ser. **83**, 105 (1987).

49. G. Brunthaler, K. Ploog, and W. Jantsch, Phys. Rev. Lett. **63**, 2276 (1989).

50. K.A. Katchaturyan, D.D. Awschalom, J.R. Rozen, and E.R. Weber, Phys. Rev. Lett. **63**, 1311 (1989).

51. S. Katsumoto, N. Matsunaga, Y. Yoshida, K. Sugiyama, and S. Kobayashi, in *Proceedings of ICPS*-20, edited by E.M. Anastassakis and J.D. Joannopoulos (World Scientific, Singapore, 1990), p. 481.

52. J. Dąbrowski and M. Scheffler, Materials Science Forum **38-41**, (Trans Tech Publications, Switzerland, 1989) p. 51.

53. H.P. Hjalmarson, P. Vogl, D.J. Wolford, and J.D. Dow, Phys. Rev. Lett. **44**, 810 (1980).

54. M. Scheffler, in *Festkörperprobleme XXII (Advances in Solid State Physics)*, edited by P. Grosse (Vieweg, Braunschweig, 1980), p. 115.

55. M. Scheffler, F. Beeler, O. Jepsen, O. Gunnarsson, O.K. Andersen, and G.B. Bachelet, in *Proceedings of the 13th International Conference on Defects in Semiconductors*, edited by L.C. Kimerling and J.M. Parsey, Jr. (The Metallurgical Society of AIME, New York, 1984), p. 45.